

Highlights

UDA4Inst: Unsupervised Domain Adaptation for Instance Segmentation

Yachan Guo, Yi Xiao, Danna Xue, Jose L. Gómez, Antonio M. López

- **Semantic Category Training:** We present a novel training strategy for instance segmentation that groups semantically related classes and trains specialized models for each group, yielding better performance than a single model trained on all classes simultaneously.
- **Bidirectional Mixing Training:** We develop a bidirectional cross-domain mixing approach, which includes patch-wise and instance-wise strategies to mitigate bias, avoid catastrophic forgetting. By adaptively choosing between instance-wise or patch-wise mixing, handling overlapping masks, aligning color spaces, and rebalancing rare classes, our method effectively tackles the domain gap and enhances instance segmentation performance across synthetic and real-world datasets.
- **Raising Performance:** Our UDA4Inst framework establishes a new state-of-the-art on the SYNTHIA → Cityscapes benchmark with mAP 31.3, improving by 6.7 points with respect to the baseline and 15.6 points to the previous state-of-the-art method.
- **Establishing New Cross-Domain Benchmarks:** We design additional novel cross-domain settings with UrbanSyn and Synscapes as synthetic source datasets and Cityscapes and KITTI360 as a real-world target, broadening the scope for future research.

UDA4Inst: Unsupervised Domain Adaptation for Instance Segmentation

Yachan Guo^a, Yi Xiao^a, Danna Xue^a, Jose L. Gómez^a, Antonio M. López^{a,b}

^a*Computer Vision Center, 08193, Barcelona, Spain*

^b*Universitat Autònoma de Barcelona, 08193, Barcelona, Spain*

Abstract

Instance segmentation is crucial for autonomous driving but is hindered by the lack of annotated real-world data due to expensive labeling costs. Unsupervised Domain Adaptation (UDA) offers a solution by transferring knowledge from labeled synthetic data to unlabeled real-world data. While UDA methods for synthetic to real-world domains (synth-to-real) show remarkable performance in tasks such as semantic segmentation and object detection, very few have been proposed for instance segmentation in vision-based autonomous driving. Moreover, existing methods rely on suboptimal baselines, which severely limits performance. We introduce **UDA4Inst**, a powerful framework for synth-to-real UDA in instance segmentation. Our framework enhances instance segmentation through *Semantic Category Training* and *Bidirectional Mixing Training*. With the Semantic Category Training method, semantically related classes are grouped and trained separately, enabling the generation of higher-quality pseudo-labels and improved segmentation performance. We further propose a bidirectional cross-domain data mixing strategy that combines instance-wise and patch-wise mixing techniques to effectively utilize data from both source and target domains, producing realistic composite images that improve the model’s generalization performance. Extensive experiments demonstrate the effectiveness of our methods. Our approach establishes a new state-of-the-art on the SYNTHIA → Cityscapes benchmark with mAP 31.3. Notably, we are the first to report results on multiple novel synth-to-real instance segmentation datasets, using UrbanSyn and Synscapes as source domains while Cityscapes and KITTI360 serve as target domains. *

*Our code will be released soon.

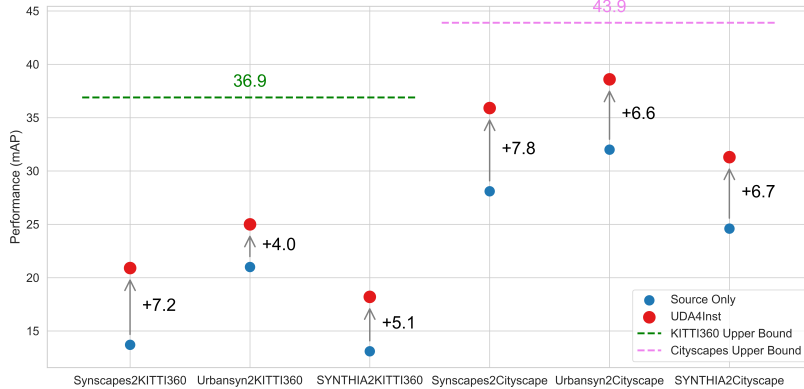


Figure 1: Instance segmentation performance across various domain adaptation scenarios. The dashed lines indicate the upper-bound models (trained on human-annotated target data), while the vertical arrows illustrate how UDA4Inst (red dots) improves upon the source-only baseline (blue dots).

Keywords:

Synth-to-Real Unsupervised Domain Adaptation, Instance Segmentation, Vision-based Autonomous Driving

1. Introduction

Instance segmentation provides a detailed and fine-grained understanding of the objects in an image. This level of precision is critical for a variety of real-world applications, such as multi-object tracking [1, 2, 3], pose estimation [4, 5], and motion prediction [6, 7]. Specifically, in autonomous driving, instance segmentation is useful as it helps to locate safety-critical objects (such as pedestrians or riders) with accurate boundaries, enabling more advanced scene analysis and decision-making in many scenarios [8, 9, 3, 10]. However, in practice, training instance segmentation models requires access to a large amount of dense manual labeled data rich in scenarios and object variability. Each instance should be accurately delineated with pixel-level masks, which is laborious and time-consuming. Therefore, the label acquisition and object variability needed for instance segmentation encounter a data-hungry bottleneck.

As an alternative, synthetic data are used to train deep models for vision tasks [11], as it offers large-scale labeled data directly generated by simula-

tors [12, 13]. Crucially, this approach enables us to generate scenarios and events rarely encountered in real-world data (e.g., densely populated scenes, accidents, borderline situations), while also providing detailed annotations almost instantly. However, when we apply models trained with synthetic data in the real-world domain, the results are often unsatisfactory due to the inevitable domain gap between them. Unsupervised Domain Adaptation (UDA) methods are essential for mitigating this inherent synth-to-real gap, where we only have access to labeled synthetic data.

In recent years, many studies have explored the integration of synthetic data and UDA methods to address a wide range of computer vision tasks including image classification [14, 15, 16, 17, 18], object detection [19, 20, 21, 22, 23, 24], and semantic segmentation [25, 26, 27, 28, 29, 30, 31]. Comparatively, there is a significant gap in its application to instance segmentation for autonomous driving. The few existing methods are constrained by sub-optimal architectures, reflected in only three works [32, 33, 34] in the last five years. Among them, although [33, 34] do provide results on instance segmentation, they worked on models designed for panoptic segmentation tasks, and [32] was based on Mask R-CNN framework with adversarial learning.

In this paper, we propose UDA4Inst, a framework for **UDA for Instance Segmentation**, employing a teacher-student online self-training approach that generates trustworthy pseudo-labels from an unlabeled target dataset.

First, we design a semantic category training approach, where we categorize the instance classes by a criterion to train more specialized models. These models use Mask2Former [35] to ensure up-to-date strong instance segmentation baselines. We combine the outputs of these specialized models to obtain better-quality instance masks that will improve the pseudo-labeling generation of our framework.

Next, we apply a bidirectional domain mixing training strategy to provide accurate pseudo-labels from the selected target domain. Unlike previous models [15, 27, 1] that limited the cross-domain data mixing to a single direction, either source-to-target (S2T) or target-to-source (T2S), UDA4Inst combines and balances both the strategies accurately to address the instance segmentation and provide the pseudo-labels.

Our S2T phase is straightforward that synthetic labeled instances are added to the target images. For the T2S phase, we generate pseudo-labels from real-world instances and accommodate them into synthetic images. Applying both strategies, we aim to mitigate any bias introduced by the source or target data and possible catastrophic forgetting during the training.

Note that one of the most challenging scenarios in instance segmentation is when multiple instances of the same class overlap. In semantic segmentation, these overlapping instances are treated as a single blob. In contrast, instance segmentation methods need to find clear boundaries in the overlapping region of objects to separate them.

Our method faces this challenge by adopting an instance-wise mixing strategy for large-area instances, ensuring that composite images retain clear object boundaries. For smaller instances, we use a patch-wise mixing method, ensuring that the instances in the mixed images retain the surrounding environmental context. This prevents small, indistinct objects from appearing abruptly or unnaturally in the new domain images. Additionally, to address instance imbalance, UDA4Inst incorporates a straightforward online algorithm that balances rare-class instances during data mixing between domains.

Finally, as a good practice, we evaluate the quality of the pseudo-labels generated by our system, using them exclusively to train a vanilla model in a supervised fashion on their respective target dataset.

We demonstrate the effectiveness of UDA4Inst on multiple UDA instance segmentation benchmarks. On SYNTHIA [36] → Cityscapes, we achieve state-of-the-art results. To the best of our knowledge, this is the first report performing UDA instance segmentation using the synthetic driving scene datasets UrbanSyn [37] and Synscapes [38], achieving 38.6 mAP and 35.9 mAP on Cityscapes [8] and 25.0 mAP and 19.5 mAP on KITTI360 [39]. Compared to the source-only method, our approach demonstrates substantial improvements across these benchmarks as in **Fig. 1**. Our contributions are as follows:

- **Semantic Category Training:** We propose a novel training strategy for instance segmentation that groups semantically related classes and trains specialized models for each group, yielding better performance than a single model trained on all classes simultaneously.
- **Bidirectional Mixing Training:** We develop a bidirectional cross-domain mixing approach, which includes patch-wise and instance-wise strategies to mitigate bias and avoid catastrophic forgetting. By adaptively choosing between instance-wise or patch-wise mixing, handling overlapping masks, aligning color spaces, and rebalancing rare classes, our method effectively tackles the domain gap and enhances instance segmentation performance across synthetic and real-world datasets.

- **Raising Performance:** Our UDA4Inst framework establishes a new state-of-the-art on the SYNTHIA → Cityscapes benchmark with mAP 31.3, improving by 6.7 points with respect to the baseline and 15.6 points to the previous state-of-the-art method.
- **Establishing New Cross-Domain Benchmarks:** We establish additional novel cross-domain settings with UrbanSyn and Synscapes as synthetic source datasets and Cityscapes and KITTI360 as a real-world target, broadening the scope for future research.

2. Related Work

2.1. Instance Segmentation

Early mainstream deep learning models based on convolutional neural networks (CNNs) for instance segmentation, such as Mask R-CNN [40] and YOLACT [41], have achieved remarkable successes. In recent years, with the adoption of the self-attention mechanism in natural language processing [42] and computer vision, [43, 44, 45] transformer-based models [46, 35, 47, 48] have emerged and surpassed CNN-based architectures in many tasks such as object detection [47], semantic segmentation [46, 35], and panoptic segmentation. [34, 35]. Among them, Mask2Former [35] has attracted great attention as a universal transformer-based architecture that obtains top results in three major image segmentation tasks (panoptic, instance, and semantic) on several benchmarks. It introduces masked attention, which extracts localized features by constraining cross-attention within predicted mask regions. In this work, we leverage this advanced universal segmentation architecture to prompt the state-of-the-art results in instance segmentation with UDA.

2.2. Unsupervised Domain Adaptation

Typically, UDA methods occupy three groups: domain discrepancy alignment, adversarial learning, and self-training. In domain discrepancy alignment, a proper divergence measure, such as maximum mean discrepancy [49], correlation alignment [50], or Wasserstein distance [51] is chosen to minimize domain discrepancy in a latent feature space. Adversarial learning approaches [52, 53, 54, 55, 56, 57] aim to achieve domain invariance in input space, feature extraction, or output space. To reduce domain discrepancy, self-training methods [26, 27, 58] train a model using a combination of labeled and unlabeled data. These methods generate high-confidence pseudo-labels

from unlabeled data and iteratively incorporate them to expand the labeled data during training, gradually improving the model’s performance. HRDA [27] enhances domain adaptation performance through the integration of hierarchical attention and multi-resolution representations. MIC [58] leverages masked image consistency to enhance context understanding for generalization. Our proposed solution follows the pattern of **self-training** since it is the mainstream approach in state-of-the-art UDA methods, and is most suitable for our bidirectional mix strategy.

Current UDA works [26, 27, 28, 29, 30, 31] mainly focus on the semantic segmentation task that is getting close to the supervised learning methods trained on human labeling datasets. On the other hand, UDA panoptic segmentation is yet to be thoroughly explored, where few works [33, 34] can simultaneously achieve domain-adaptive instance and semantic segmentation within a single network. The work most related to ours is [32], which proposes a multi-level feature adaptation strategy to improve synth-to-real instance segmentation. To reduce the domain gap, they focus on aligning feature distributions between synthetic and real data at global, local, and subtle levels. This is achieved by using Mask R-CNN and discriminator networks with adversarial learning. In recent years, there has been significant progress in the research fields of non-cross-domain instance segmentation and UDA methods. In this work, we aim to improve the baseline on UDA for instance segmentation with approaches such as cross-domain data mixing along with the advanced transformer-based Mask2Former network.

2.3. Cross-domain Data Mixing

A commonly used data augmentation technique is mixing image content. In UDA, this augmentation is usually applied in the form of cross-domain mixing, *i.e.* the mixed samples consist of data from both source and target domains. Tranheden *et al.* introduce DACS [59], a unidirectional cross-domain data mixing strategy that cuts out semantic classes in the source domain and pastes them into samples in the target domain. Suhyeon *et al.* use a similar method by transferring the tail-class content from source to target to solve the class imbalance problem [60]. Gao *et al.* propose a dual soft-paste strategy that not only considers mixing from the source to target images but also within the source domain itself [61]. A similar idea is suggested by Huo *et al.*, while for the dual mixing [62], they focus on the target-to-target domain. Most recently, Kim *et al.* proposed a S2T and

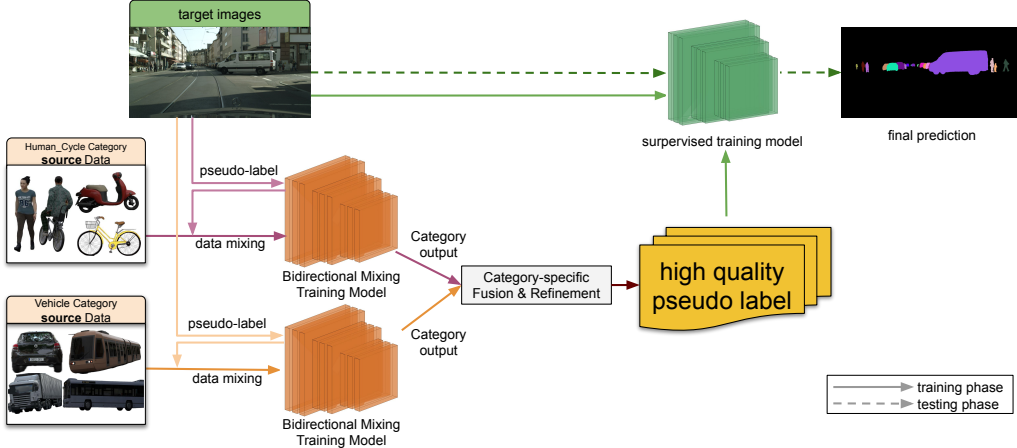


Figure 2: Overview of the UDA4Inst framework pipeline. The source data is initially divided into two categories: human-cycle and vehicle. Each category undergoes independent training to produce specialized models capable of generating pseudo-labels for the target domain. The category-specific labels from the source and the pseudo-labels from the target domain are then used to perform the bidirectional mixing training. The outputs of these models are subsequently fused and refined to generate high-quality pseudo-labels. These pseudo-labels, along with target domain images, are used for supervised training to produce the final predictions in the target domain. The process is divided into the training phase (solid arrows) and the testing phase (dashed arrows).

T2S cut-and-paste strategy based on predefined image patches [63]. It is noteworthy that these mixing approaches fall into two categories:

(1) *Class-wise Mixing*. For instance, Cardace *et al.* [64] only mix semantic classes such as ‘Car’, ‘Person’, and ‘Pole’. This approach fails to delineate boundaries accurately where multiple instances overlap.

(2) *Random Patches Mixing*. This approach involves cut-and-paste based on arbitrary patches, resulting in unrealistic images with mixed foreground instances and background area.

Unlike the prior works in semantic segmentation, we develop a bidirectional domain mixing strategy for both S2T and T2S mixing instance-wise and patch-wise. In addition, to create more realistic composite images and enhance the model’s generalization capabilities, we use an instance-wise strategy for mixing larger instances, ensuring clear contours and a natural appearance. For smaller instances, a patch-wise mixing method is applied, allowing them to seamlessly integrate into the surrounding environment without appearing out of place, even in the new domain images.

3. Methodology

3.1. Overall Approach

Our paper introduces the UDA4Inst framework. **Fig. 2** provides an overview of the pipeline. In this method, we perform Semantic Category Training by dividing the training data into several related semantic groups, (e.g. **Human-Cycle** and **Vehicle**). We train an individual model for each group. Moreover, we apply the bidirectional mixing training, which involves cross-domain cut-and-paste operations performed both instance-wise and patch-wise to train the model. The outputs of these models are subsequently fused and refined to generate high-quality pseudo-labels from the unlabeled target data. Our final step uses only these pseudo-labels to train a single final model, then produce the final predictions in the target domain. This framework aims to generate high-quality pseudo-labels, which are then used to train with the target domain data in a supervised manner, ultimately producing the final instance segmentation results. After an overall explanation of our UDA4Inst framework, we explain in more detail our key proposals: Semantic Category Training and Bidirectional Mixing Training.

3.2. Semantic Category Training

Instance labels inherently carry distinct semantic meanings. Classes that share similar semantics often exhibit overlapping features. For instance, motorcycles and bicycles display a higher degree of feature similarity compared to trains and bicycles, reflecting closer semantic affinity among certain classes. Drawing from our empirical observations, we hypothesize that introducing an inductive bias by grouping semantically similar classes can guide the model to more effectively learn both inter-class and intra-class features. Consequently, we propose organizing similar classes into groups and training specialized models for each group to enhance segmentation performance by generating more accurate pseudo-labels in the target domain. In this study, we categorize the eight instance classes into two distinct groups: (1) Human-Cycle, comprising person, rider, bicycle, and motorcycle; and (2) Vehicle, comprising car, truck, bus, and train.

Instead of training on all classes at once, our method first groups semantically related classes for specialized training. (see Table 8). In this framework, we first train separate models, each dedicated to a subset of the class space. This category-based training strategy ensures that each model

refines its internal representations for a distinct group of classes. We extend this methodology from synthetic datasets to more complex real-world datasets such as Cityscapes and KITTI360, applying the same principle of focused class grouping.

Building on this strategy, we integrate the category-based approach into an unsupervised domain adaptation (UDA) pipeline. Within the UDA framework, two specialized models are initially trained in parallel, each model responsible for a different set of classes. Their outputs are subsequently fused to produce pseudo-labels for the target domain. The fusion mechanism involves confidence-based assessments of each model’s output, merging segmentation results at the class level and ensuring that each instance is attributed to one model. By concentrating on distinct class groups, our method promotes robust feature representations and generates higher-quality pseudo-labels for the target domain. Detailed comparisons of full-class and category-driven strategies, as well as ablation studies, are provided in Section 4.4.4.

3.3. Bidirectional Mixing Training

On each of the two categories, we apply our Bidirectional Mixing Training. Where the source domain dataset \mathcal{D}_S , comprising images X_S , their instance labels Y_S , an instance segmentation model f_θ ; is trained in a supervised manner. The target domain dataset \mathcal{D}_T only provides images X_T . We aim to address the domain gap by leveraging X_S , Y_S , and X_T to train a model capable of accurately segmenting instances on X_T .

As shown in **Fig. 3**, our UDA method is based on online self-training. The training has two stages. In the first stage, the model f with parameters θ is trained on the source domain in a supervised manner for T_{stage1} iterations, with synthetic images X_S and their corresponding ground-truth labels Y_S , to generate predictions \hat{Y}_S . Our goal is to minimize a supervised segmentation loss

$$\mathcal{L}_{stage1} = \mathcal{L}_{seg}(\hat{Y}_S, Y_S), \quad (1)$$

then the network can be used to predict pseudo-labels, \hat{Y}_T , on the target domain. In our case, we use the aforementioned Mask2Former as the base network for instance segmentation. The segmentation loss for Mask2Former is

$$\mathcal{L}_{seg} = \lambda_{ce}\mathcal{L}_{ce}(\hat{Y}, Y) + \lambda_{bce}\mathcal{L}_{bce}(\hat{Y}, Y) + \lambda_{dice}\mathcal{L}_{dice}(\hat{Y}, Y), \quad (2)$$

where binary cross-entropy loss \mathcal{L}_{bce} and dice loss \mathcal{L}_{dice} are for binary mask segmentation, \mathcal{L}_{ce} is for instance class classification. λ_{bce} , λ_{dice} and λ_{ce} are

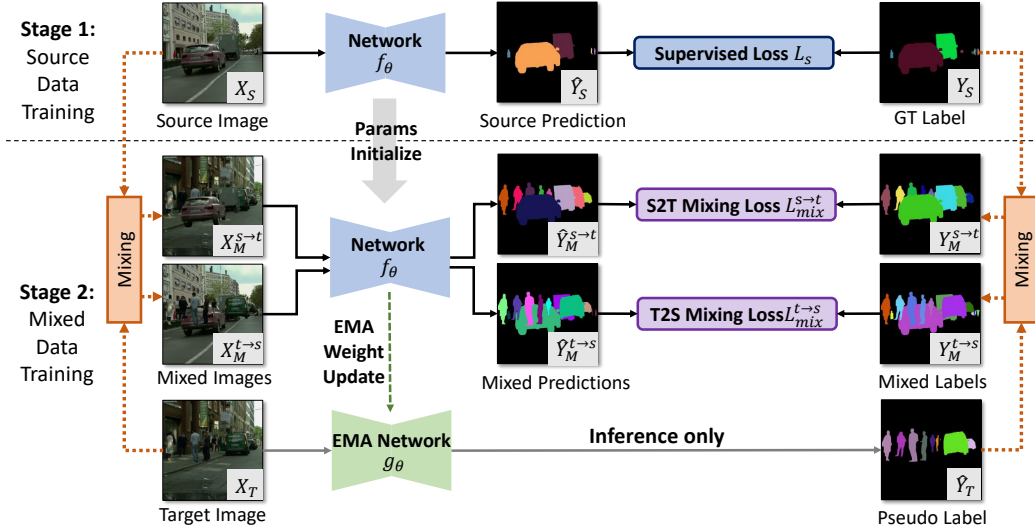


Figure 3: Pipeline of mixing training module. In the first stage, the student network is trained with source domain data in a supervised manner. In each iteration of the second stage, we update the EMA teacher g_θ with the weights from the network f_θ to predict pseudo-labels in the target domain. Next, the mixed data are generated with the source and target images, and the mixed labels are generated by the target pseudo-labels and the source ground-truth labels. The network is then trained on the mixed data with S2T and T2S mixing losses.

weighting hyper-parameters.

In the second stage, we utilize the images and labels produced by our bidirectional cross-domain mixed approach on source and target domain data to resume the training of the model f_θ for T_{stage2} iterations. Since the target images X_T are unlabeled, we utilize the pseudo-labels generated by the exponential moving average (EMA) teacher model g_θ . At the beginning of the second stage, the parameters of the EMA teacher are initialized by the weights of f_θ . Then, in each training step, we first infer the target images by the EMA teacher to get pseudo-labels \hat{Y}_T . In line with common practice [59, 27, 26, 58], we use confidence thresholds to filter out noisy pseudo-labels. A pseudo-label confidence score is defined as the product of *mask confidence* (confidence of whether an instance object exists in a mask) and *class confidence* (confidence of an instance class). Then, we leverage the ground-truth labels Y_S and the pseudo-labels \hat{Y}_T to perform bidirectional instance cut-and-paste, thereby obtaining mixed data $X_M^{s \rightarrow t}$, $Y_M^{s \rightarrow t}$, $X_M^{t \rightarrow s}$, $Y_M^{t \rightarrow s}$. Finally, mixed data are used to train the model f_θ with a weighted bidirectional data mixing

Algorithm 1 Bidirectional Mixing Training

Require: Source domain datasets $\{X_S^i, Y_S^i\}_{i=1}^{N_S}$, target domain dataset $\{X_T^j\}_{j=1}^{N_T}$, iterations for stage1 and stage2 T_{stage1} , T_{stage2} , instance segmentation model f_θ , and EMA teacher model g_θ

- 1: **for** $iter = 1$ to $iter = T_{stage1}$ **do** ▷ Stage 1: source data training
- 2: Compute prediction, $\hat{Y}_S \leftarrow f_\theta(Y_S)$.
- 3: Compute supervised loss, $\mathcal{L}_{stage1}(\hat{Y}_S, Y_S)$.
- 4: Compute gradients, $loss.backward()$.
- 5: Update f_θ weights, $optimizer.step()$.
- 6: **end for**
- 7: **for** $iter = 1$ to $iter = T_{stage2}$ **do** ▷ Stage 2: mix data training
- 8: Update the parameters of EMA teacher $g_\theta \leftarrow f_\theta$.
- 9: Generate pseudo-labels for target images $\hat{Y}_T \leftarrow g_\theta(X_T)$.
- 10: Generate mixing images and labels $X_M^{s \rightarrow t}, Y_M^{s \rightarrow t}, X_M^{t \rightarrow s}, Y_M^{t \rightarrow s} \leftarrow$ Augmentation, bidirectional mixing X_S, Y_S, X_T, \hat{Y}_T , and rare class sampling
- 11: Compute prediction, $\hat{Y}_M^{s \rightarrow t} \leftarrow f_\theta(X_M^{s \rightarrow t})$, $\hat{Y}_M^{t \rightarrow s} \leftarrow f_\theta(X_M^{t \rightarrow s})$.
- 12: Compute mix losses, $\mathcal{L}_{stage2}(\hat{Y}_M^{s \rightarrow t}, \hat{Y}_M^{t \rightarrow s}, Y_M^{s \rightarrow t}, Y_M^{t \rightarrow s})$.
- 13: Compute gradients, $loss.backward()$.
- 14: Update f_θ weights, $optimizer.step()$.
- 15: **end for**
- 16: **return** f_θ

loss

$$\mathcal{L}_{stage2} = \lambda_{mix}^{s \rightarrow t} \mathcal{L}_{seg}(\hat{Y}_M^{s \rightarrow t}, Y_M^{s \rightarrow t}) + \lambda_{mix}^{t \rightarrow s} \mathcal{L}_{seg}(\hat{Y}_M^{t \rightarrow s}, Y_M^{t \rightarrow s}), \quad (3)$$

where $\lambda_{mix}^{s \rightarrow t}$ and $\lambda_{mix}^{t \rightarrow s}$ are weights for different directional mixing data. Then, the EMA teacher parameters are updated. Algorithm 1 illustrates the implementation of the Bidirectional Mixing Training in detail.

In data mixing, the mixed images are generated by cut-and-paste image regions from one image to another in a similar fashion to [65]. We adopt a bidirectional mixing strategy that fully utilizes instances from both source and target domains to facilitate instance segmentation. As shown in **Fig. 4**, in each iteration of this training stage, the mixed data is generated in both directions: source to target (T2S) and target to source (T2S). For S2T mixing, the instances in a source domain image X_S are cut and pasted onto a target domain image X_T , resulting in an augmented mixing images $X_M^{s \rightarrow t}$. Its corresponding instance label $Y_M^{s \rightarrow t}$ is created according to the image, where the

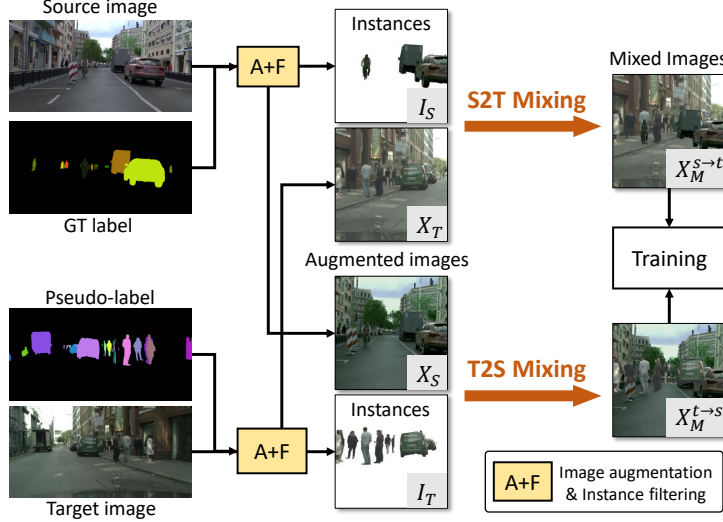


Figure 4: Bidirectional data mixing for instance segmentation. The mixed images and labels are generated by cutting the instances from either the source or target domain, and pasting them to images in another domain.

instance labels are added to the generated target pseudo-labels \hat{Y}_T . Similarly, to obtain the T2S mixing data $X_M^{t \rightarrow s}$ and $Y_M^{t \rightarrow s}$, we leverage the generated pseudo-labels of the target images \hat{Y}_T to get the instances that are desired to be pasted on the source image X_S . The network is trained on mixed images $X_M^{s \rightarrow t}$, $X_M^{t \rightarrow s}$ with mixed labels $Y_M^{s \rightarrow t}$, $Y_M^{t \rightarrow s}$.

3.3.1. Combining Instance-wise and Patch-wise Strategies

In our bidirectional data mixing strategy, we adaptively choose between instance-wise and patch-wise mixing based on the size of the instances. Specifically, if the area of an instance exceeds a certain threshold, we apply instance-wise mixing. This allows us to paste larger instances onto new backgrounds while preserving clear contours and details, resulting in more realistic composite images. Conversely, for instances whose area is smaller than the threshold, we utilize patch-wise mixing. Small objects often have blurry appearances and unclear boundaries, which makes it difficult to segment them accurately. When such inaccurate small instances are extracted from their original background and pasted into a new domain, they may become difficult to discern due to the lack of contextual information, bringing error to the pseudo-label. In **Fig. 5**, we show an example of the instance-wise and patch-wise combined strategy for different instance sizes. The big



Figure 5: Mixing Strategy. This figure presents the instance-wise and patch-wise combined strategy for different instance sizes from the source image to the target image. **Red** bounding box indicates the instance-wise mixing, and **Green** one indicates the patch-wise mixing.

rider is mixed with instance-wise and the small person is mixed patch-wise with a rectangular area. By using patch-wise mixing, we include not only the small instances but also some surrounding context from the original image. This helps maintain visual coherence and reduce instance inaccuracies in the composite images.

In addition, during this strategy, we apply the next mechanisms to address common problems such as overlapping inconsistencies, color discrepancies between source and target images, and class imbalance during the cut-and-mix selection.

3.3.2. Overlapping Strategy

Overlapping instances in mixing process between source and target domains can create ambiguous labels and unrealistic visual artifacts, potentially confusing the model during training. To address this, we implement a priority masking strategy. Specifically, in S2T mixing, we assign higher priority to the source domain instances. If an instance from the source image X_S overlaps with an instance in the target image X_T , we erase the overlapping region of the target's instance labels \hat{Y}_T , keeping only the source instance in that region. This means that the source instance's mask replaces any conflicting target instance masks in the overlapping area. We do a similar strategy for T2S mixing.

3.3.3. Color Space Transfer

To minimize the color discrepancy, we adopt the same image processing as [30], aligning the style of source domain images to the target ones by shifting the distribution of pixel values in CIELAB color space.

3.3.4. Rare-class Balancing

Class imbalance is a common issue that affects the performance of deep learning models. Models trained on imbalanced datasets tend to favor classes with more data, leading to lower accuracy in classes with fewer examples. This problem exists in the three synthetic datasets we use. Therefore, we increase the training frequency of these rare class instances by intentionally resampling them in data mixing. In each category group, for the class that occupies the smallest percentage of instances in the source dataset, we define it as a rare class. For example, in UrbanSyn, ‘Motorcycle’ and ‘Train’ are 2.47% and 0.37%. Specifically, during the process of traversing images for data mixing, for those images containing rare-class instances, we store these images and the corresponding instance labels in a pool with a maximum number of N . These samples are continuously updated with newly emerged rare-class instances and their corresponding images in a FIFO (first-in, first-out) fashion. In turn, when encountering images that do not contain rare classes, we randomly select half of the samples in the pool and mix them on these images. To avoid error accumulation from pseudo-labels, we only apply rare-class balancing to data mixing in the S2T direction.

4. Experiments

4.1. Datasets

In this work, we perform experiments across comprehensive synthetic-to-real domain settings. We selected SYNTHIA [36], Synscapes [38] and UrbanSyn [37] as synthetic datasets and Cityscapes [8] and KITTI360 [39] as real-world datasets.

UrbanSyn is a high-quality synthetic dataset tailored to urban driving scenarios. It comprises a total of 7,539 images with a resolution of 2048×1024 pixels and has the same instance and semantic classes as Cityscapes. **Synscapes** includes 25,000 images at a resolution of 1440×720 . The labeled data covers 8 instance classes, but the division is different from Cityscapes. To make them consistent with Cityscapes, we reclassify the ‘Motorcyclist’ and ‘Bicyclist’ instances into ‘Motorcycle’, ‘Bicycle’, and ‘Rider’ leveraging

semantic labels. **SYNTHIA** consists of images in a resolution of 960×720 rendered from a virtual city, with a subset compatible with Cityscapes. This subset contains 9,400 images with pixel-level semantic annotations. SYNTHIA covers 6 classes of instance annotation in Cityscapes, missing ‘Train’ and ‘Truck’.

Cityscapes is a street-scene dataset that contains 5000 images (2,975, 500, and 1,525 images for training, validation, and testing, respectively) and their corresponding labels for 19 semantic classes and 8 instance classes. Cityscapes is a commonly used real-domain dataset with high-resolution (2048×1024) images in the field of autonomous driving. **KITTI360** consists of 9 training sequences and 1 validation sequence, covering diverse scenarios such as urban streets and rural roads. The images have a resolution of 1408×376 pixels.

4.2. Implementation Details

4.2.1. Training

We adopt Mask2Former [35] with Swin Transformer backbone [31] as our base network f_θ . The model is pre-trained on COCO [66] dataset. We apply the same data augmentation (flipping, random cropping, *etc.*) as [35] and set the image crop size to 1024×1024 when the target domain is Cityscapes and 384×672 for KITTI360. The maximum number of samples N for the rare-class pool is set to 10, and the pseudo-label confidence threshold τ is 0.9. We set the numbers of iterations for source domain training T_{stage1} to 40k, while the mixed data training T_{stage2} is 40k iterations. During validation, we follow the same checkpoint selection protocol used in [58]. For each stage of training, we set a batch size $B=3$ considering optimal memory usage. We use AdamW [67] optimizer with an initial learning rate of 0.0001 and a weight decay of 0.05, as well as the ‘poly’ learning rate schedule with the power of 1. The hyper-parameters of loss λ_{bce} , λ_{dice} , and λ_{ce} are set to 5.0, 5.0, 2.0 respectively. During the supervised training phase using pseudo-labels, we adopt the same training configuration. For bidirectional mixing, we set the pixel area threshold to 1500: instances with an area larger than this threshold are processed instance-wise, while those below are handled patch-wise. For these experiments, UDA4Inst runs on 1 NVIDIA A40 GPU with 48GB of memory.

Methods	AP												AP50											
	Person	Rider	Car	Truck	Bus	Train	M.bike	Bike	mAP	Imp.	Person	Rider	Car	Truck	Bus	Train	M.bike	Bike	mAP50	Imp.				
Cityscapes supervised	41.1	32.4	61.4	44.8	67.5	50.7	26.8	26.6	43.9	-	75.4	71.3	87.2	58.7	80.3	76.1	58.1	65.1	71.5	-				
UrbanSyn → Cityscapes																								
Source only	25.1	19.5	39.8	37.6	51.5	46.7	19.2	16.2	32.0	-	52.0	48.4	61.5	48.6	66.2	70.0	42.6	46.0	54.4	-				
UDA4Inst	30.4	26.6	48.8	46.3	63.0	51.6	22.7	19.4	38.6	+7.0	63.1	62.4	75.7	57.3	76.3	80.1	50.9	54.8	65.1	+9.4				
Synscapes → Cityscapes																								
Source only	27.2	19.2	39.5	24.0	46.7	33.1	18.7	16.6	28.1	-	53.9	44.3	67.8	31.9	60.6	58.1	39.9	45.4	50.2	-				
UDA4Inst	30.0	26.9	47.7	35.1	58.3	47.3	21.9	19.8	35.9	+7.8	60.0	63.0	78.1	44.8	72.5	62.7	46.0	51.8	59.9	+9.7				
SYNTHIA → Cityscapes																								
Source only	26.3	15.2	38.3	-	43.0	-	13.6	10.9	24.6	-	53.4	40.8	68.1	-	56.5	-	36.4	36.1	48.6	-				
UDA4Inst	28.0	19.9	46.8	-	59.5	-	18.0	15.8	31.3	+6.7	57.0	53.5	76.4	-	67.9	-	43.8	42.9	56.9	+8.3				
KITTI360 supervised	36.6	16.8	55.5	37.0	98.4	16.4	24.0	10.3	36.9	-	71.5	41.2	84.4	53.2	100.0	42.7	49.0	34.1	59.5	-				
UrbanSyn → KITTI360																								
Source only	14.0	6.8	44.2	12.0	63.5	6.7	13.6	7.0	21.0	-	44.0	33.0	75.8	19.5	66.0	15.8	36.7	19.2	38.8	-				
UDA4Inst	16.4	7.2	45.4	13.6	81.6	13.5	13.9	8.4	25.0	+4.0	55.1	33.9	76.3	20.1	83.5	28.8	38.6	21.2	44.6	+5.8				
Synscapes → KITTI360																								
Source only	15.2	5.1	44.4	6.7	17.9	0.5	14.1	6.1	13.7	-	43.4	24.7	74.4	12.6	18.6	1.3	36.5	16.6	28.5	-				
UDA4Inst	20.1	4.8	46.9	13.8	60.4	0.2	13.4	7.9	20.9	+7.2	56.8	23.9	78.5	23.9	60.6	0.9	36.4	21.8	37.9	+9.4				
SYNTHIA → KITTI360																								
Source only	3.3	2.6	32.5	-	34.1	-	2.8	3.5	13.1	-	10.0	13.5	66.2	-	37.0	-	12.3	12.7	25.3	-				
UDA4Inst	10.3	3.0	41.5	-	47.6	-	1.9	4.9	18.2	+5.1	32.1	15.4	69.4	-	47.8	-	7.4	15.6	31.3	+6.0				

Table 1: The Instance segmentation performance on UDA benchmarks. This table presents the performance improvements that provide UDA4Inst with respect to the vanilla Mask2former baseline in synth-to-real settings. ‘Imp.’ is improvement of UDA4Inst models.

4.2.2. Evaluation

We evaluate the UDA performance of 8-class instance segmentation on the validation set of Cityscapes. Following the conventional evaluation criteria of instance segmentation, we take AP (Average Precision) and AP50 (Average Precision at $IOU > 0.5$) and their mean values as our metrics for comparison. All the numbers present in the tables are in %.

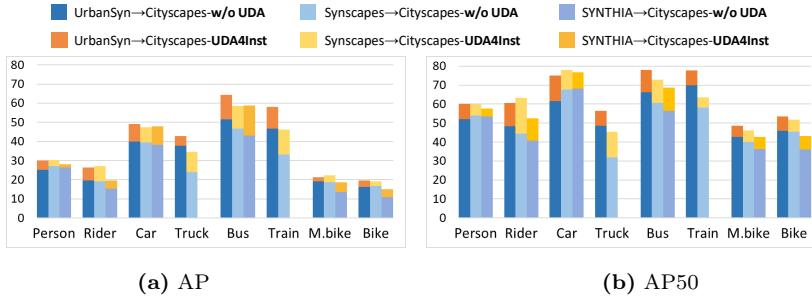


Figure 6: Comparison of class-wise AP and AP50 between UDA4Inst and the source-only model. UDA4Inst shows evident improvements (the Orange/Yellow parts) in all three synth-to-real settings.

4.3. Experimental Results

4.3.1. UDA performance

In Table 1, we summarize the performance improvements that provide UDA4Inst with respect to the vanilla Mask2former baseline in the aforementioned synth-to-real settings. In addition, at the beginning of each table block, we show the results of the supervised Mask2Former model training on Cityscapes and KITTI360 datasets as the upper bounds. UDA4Inst consistently outperforms the source-only model across all settings, significantly improving both mAP and mAP50 metrics. UDA4Inst achieves mAP of 38.6 in UrbanSyn \rightarrow Cityscapes, 35.9 in Synscapes \rightarrow Cityscapes. For SYNTHIA \rightarrow Cityscapes, our mAP is 31.3, setting a new state-of-the-art. Compared to the vanilla Mask2Former, UDA4Inst improves mAP by +7.0, +7.8, and +6.7 points for these three benchmarks respectively. We provide bar charts of class-wise AP and AP50 results for Cityscapes target in **Fig. 6** to see the gains of UDA4Inst over the source-only one. Our method achieves notable improvement in classes such as ‘Car’, ‘Truck’, ‘Bus’ and ‘Train’, while improvements on ‘Person’, ‘M.bike’ and ‘Bike’ are comparatively more modest. We suspect that larger, more rigid vehicles share more consistent features between domains, easing adaptation, whereas smaller, more deformable objects introduce higher variability and thus prove more challenging. For UrbanSyn \rightarrow Cityscapes, **Fig. 7** presents the predictions and error maps, highlighting and illustrating the performance improvements of UDA4Inst over the source-only model, while **Fig. 8** compares UDA4Inst’s performance with the upper-bound model trained on Cityscapes using human-annotated data. Moreover, UDA4Inst also delivers notable gains in KITTI360 settings, with mAP reaching 23.2 in UrbanSyn \rightarrow KITTI360 and 20.1 in Synscapes \rightarrow KITTI360, further demonstrating its adaptability across diverse domains. Note that among all the source datasets, UrbanSyn clearly achieves the best performance on both target datasets, Cityscapes and KITTI360. We attribute this performance difference to the high fidelity and photorealistic nature of this dataset, which more closely resembles the target domains. As a result, the reduced domain gap enables more effective adaptation and superior instance segmentation outcomes.

Computational Cost. Since our proposed UDA framework focuses on generating more reliable pseudo-labels for the target domain and subsequently training a model in a supervised manner, it introduces no additional computational overhead during the testing and inference stages. Table 2 presents

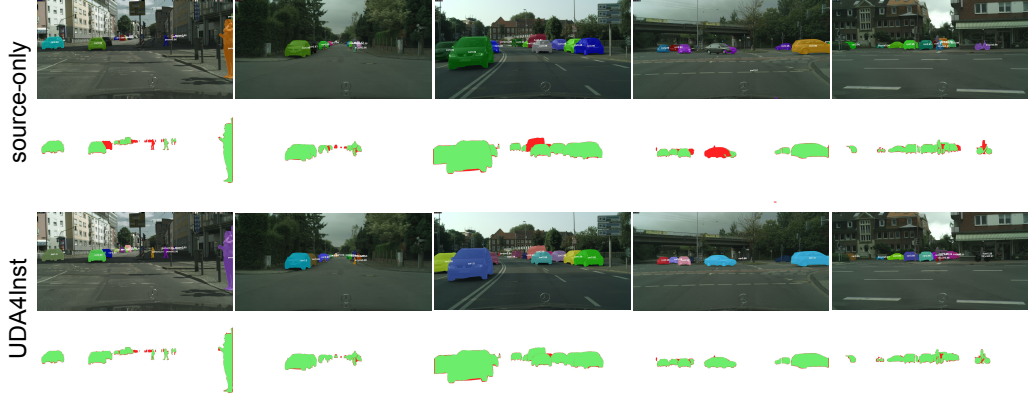


Figure 7: Qualitative comparison of instance segmentation for the source-only model and UDA4Inst for UrbanSyn → Cityscapes. We show the instance segmentation predictions on images and error maps of semantic results. **Green** indicates correct predictions, while **red** highlights errors compared to the ground truth.

the inference performance metrics for Mask2Former and UDA4Inst using the Swin-L backbone and a resolution of 1024×2048 , using 1 NVIDIA A40 GPU with 48GB of memory.

Attribute	UDA4Inst
Inference Time (ms)	467
Memory Usage (MB)	6604.03
FLOPs (G)	868

Table 2: Comparison of Model Efficiency and Resource Usage

Comparison with Previous Work. Unsupervised domain adaptation (UDA) for instance segmentation in the autonomous driving field, has received limited attention. For reference, in Table 3, we list results from Zhang [32], CVRN [33], and EDAPS [34], which have been proposed in recent years for UDA instance segmentation on the SYNTHIA → Cityscapes benchmark. To the best of our knowledge, these three works are the only published methods available for this benchmark. Zhang [32] focuses on instance segmentation using Mask R-CNN with a ResNet backbone, while CVRN [33] and EDAPS [34] address panoptic segmentation, a task that leverages more comprehensive annotations. We present these results to contextualize UDA4Inst’s perfor-

Methods	Backbone	AP										AP50									
		Person	Rider	Car	Truck	Bus	Train	M.C	B.C	mAP	Person	Rider	Car	Truck	Bus	Train	M.C	B.C	mAP50		
Zhang [32]	ResNet	9.4	3.8	22.2	-	23.5	-	3.2	2.4	10.8	28.8	17.8	39.9	-	37.5	-	12.8	11.9	24.8		
CVRN [33]	ResNet	-	-	-	-	-	-	-	-	-	34.4	25.3	38.7	-	38.1	-	10.1	8.7	25.9		
EDAPS [34]	Mix Transformer-B5	23.5	13.4	27.5	-	23.6	-	5.8	0.1	15.7	53.9	40.6	50.5	-	38.8	-	21.1	0.7	34.3		
UDA4Inst	Swin Transformer-Large	28.1	19.6	47.9	-	58.7	-	18.5	15.0	31.3	57.7	52.5	76.9	-	68.6	-	42.6	43.3	56.9		

Table 3: The Instance segmentation performance on SYNTHIA → Cityscapes.

	SCT	BMT	RcB	Person	Rider	Car	Truck	Bus	Train	M.C	B.C	mAP
M1	-	-	-	25.1	19.5	39.8	37.6	51.5	46.7	19.2	16.2	32.0
M2	✓	-	-	25.2	20.7	47.0	40.2	60.1	52.0	17.1	16.1	34.8
M3	-	✓	-	27.7	23.2	44.2	42.3	61.7	52.7	21.2	15.5	36.1
M4	✓	✓	-	28.9	27.6	50.0	43.6	63.7	47.3	19.5	20.7	37.7
M5	✓	✓	✓	30.4	26.6	48.8	46.3	63.0	51.6	22.7	19.4	38.6

Table 4: Component ablation on UDA methods.

mance relative to existing approaches, rather than to provide a strictly direct comparison.

4.4. Ablation Studies

4.4.1. Component Ablation

UDA4Inst components include Semantic Category Training (SCT), Bidirectional Mixing Training (BMT) and Rare-class Balancing (RcB). To assess the impact of these components, we perform an ablation study in the Urban-Syn → Cityscapes setting in Table 4. The ablative models are named from M1 to M5 (from top to bottom) for illustration. Overall, M1 without UDA obtains the lowest mAP of 32.0, while M6, equipped with all three UDA methods, achieves the highest score of 39.0. When comparing M1 and M2, applying SCT can effectively improve the model performance by +2.8 mAP. The conclusion is further strengthened by comparing M3 and M4. The performance jump from 32.0 to 36.1 mAP (+4.1) from M1 to M3 demonstrates the effect of BMT. Moreover, under the same circumstances as SCT, BMT helps to improve the precision in M4 across most classes compared to M2, contributing to a +2.9 mAP improvement. The RcB method, based on BMT and SCT, is applied in M5. Focusing on the defined rare classes, RcB helps M5 to obtain +10.8 and +1.8 AP gains to the M4 in ‘Train’ and ‘Motorcycle’, respectively. M4, using BMT alone without RcB, scores -1.3 mAP lower than M5. Comparing ablative models, BMT stands out as the most beneficial method for domain adaptation.

Mixing Strategy	mAP
w/o mixing	31.95
S2T mixing	36.07
T2S mixing	35.00
bidirectional mixing	37.18

Table 5: Ablation study on data mixing strategy.

Source	instance-wise	patch-wise	combined
UrbanSyn	14.8	21.9	22.7
Synscapes	15.9	12.7	20.9
SYNTHIA	12.5	13.4	18.2

Table 6: Ablation of mixing type. This table shows three mixing types, instance-wise, patch-wise, and the combination of both with three source datasets and KITTI360 as the target domain.

4.4.2. Bidirectional Mixing Training

To illustrate the advantages of Bidirectional Mixing Training (BMT), we conduct experiments on different data mixing strategies without applying Rare-class Balancing (RcB) and Semantic Category Training (SCT). The results in the UrbanSyn → Cityscapes setting are shown in Table 5. The mAP results reveal that both S2T and T2S mixing contribute to better performance. T2S is slightly inferior to S2T, which we believe is because the noise in the target pseudo-labels can inevitably cause interference in data mixing. Combining S2T and T2S mixing bidirectionally achieves the best result of 37.18 mAP, +5.23 higher than the plain model without mixing. Note that only applying S2T mixing neglects the instances in target images. Through BMT, we achieve a balance between learning target features and mitigating the negative impact of incorrect target pseudo-labels on the model. We also perform a study for the instance-wise and patch-wise mixing. The results are shown in Table 6.

4.4.3. Impact of Different Class Grouping Strategies

To evaluate the robustness and effectiveness of our class grouping strategy, we conducted an ablation study with various grouping configurations to identify the optimal strategy for maximizing segmentation performance. The

Setting	Category Groups	mAP	mAP50
1	{Person, Rider, Motorcycle, Bicycle, Car, Truck, Bus, Train}	32.0	54.4
2	{Person, Rider, Bus, Motorcycle}, {Car, Truck, Train, Bicycle}	33.9	57.8
3	{Person, Rider, Car, Bicycle}, {Truck, Bus, Train, Motorcycle}	35.0	59.4
4	{Person, Rider}, {Car, Truck, Bus, Train, Motorcycle, Bicycle}	35.1	59.3
5	{Person, Rider, Motorcycle, Bicycle}, {Car, Truck, Bus, Train}	35.5	59.4

Table 7: Ablation study on Semantic Category Training. The category groups are defined by classes in brackets.

experimental results are presented in Table 7. In the UrbanSyn → Cityscapes setting, we compared four grouped-class models (Settings 2-5) against the full-class model (Setting 1). All grouped-class models outperformed the full-class model, with Setting 5 achieving the highest improvement of +3.5 mAP. This validates our hypothesis that semantic similarity-based grouping enhances feature learning and reduces inter-class confusion, thereby improving segmentation accuracy and the quality of pseudo-labels. Specifically, Setting 5 groups Person, Rider, Motorcycle, Bicycle and Car, Truck, Bus, Train, providing a balanced and semantically coherent division of classes. In contrast, Setting 2 groups Person, Rider, Bus, Motorcycle and Car, Truck, Train, Bicycle, which introduces semantic overlap between Bus and Motorcycle. This overlap increases inter-class confusion, resulting in less significant performance gains compared to Setting 5.

Overall, the ablation study underscores the critical role of semantic similarity in class grouping. By organizing classes into semantically coherent groups, our approach significantly enhances segmentation performance and domain adaptation effectiveness, demonstrating the superiority of semantic similarity-based class grouping strategies in instance segmentation tasks and offering a promising direction for future research.

4.4.4. Semantic Category Training

To validate our hypothesis that grouping semantically similar classes can guide the model to produce better pseudo-labels, we conducted a comprehensive comparison between two Mask2Former-based instance segmentation models: the full-class model and the category model. The first approach trains on all eight instance classes simultaneously, while the second trains separately on two semantically related class groups: Human Cycle (person, rider, bicycle, motorcycle) and Vehicle (car, truck, bus, train).

Eval. Setting	AP										AP50										
	Person	Rider	Car	Truck	Bus	Train	M.C	B.C	Avg.	Imp.	Person	Rider	Car	Truck	Bus	Train	M.C	B.C	Avg.	Imp.	
Src	Urbansyn full-class	29.9	44.1	65.9	73.0	65.1	-	40.4	36.6	50.7	-	63.6	76.2	89.3	90.5	88.2	-	74.0	78.6	80.1	-
	Urbansyn category	48.1	46.7	71.0	79.4	68.9	-	44.0	40.6	57.0	6.3	83.4	79.4	91.3	96.6	90.1	-	78.5	82.6	86.0	5.9
	Synscapes full-class	47.3	50.4	59.9	57.3	57.2	50.0	43.7	40.9	50.8	-	83.1	89.5	86.8	84.8	82.3	77.3	87.5	84.0	84.4	-
	Synscapes category	45.6	48.0	61.7	60.6	61.0	55.4	43.0	42.4	52.2	1.4	81.2	87.7	88.5	88.4	87.3	83.9	86.2	85.4	86.1	1.7
	SYNTHIA full-class	23.1	23.3	39.9	-	40.9	-	28.5	10.5	27.7	-	54.1	60.8	64.6	-	63.4	-	60.4	37.7	56.8	-
	SYNTHIA category	28.3	23.7	52.1	-	57.3	-	29.3	10.9	33.6	5.9	61.8	62.7	82.1	-	85.6	-	62.2	39.9	65.7	8.9
CS	Urbansyn full-class	15.4	20.3	41.7	38.9	58.0	47.1	19.2	14.5	31.9	-	37.6	49.7	68.6	50.6	74.3	74.2	46.2	43.4	55.6	-
	Urbansyn category	25.3	22.5	45.8	42.5	61.3	45.2	19.6	15.8	34.8	2.9	54.9	56.5	71.3	53.8	74.1	62.2	44.8	47.0	58.1	2.5
	Synscapes full-class	25.9	18.3	42.9	29.2	44.5	29.5	15.1	11.9	27.1	-	54.3	41.5	70.9	37.2	56.9	43.6	37.5	37.8	47.5	-
	Synscapes category	27.5	19.2	46.5	22.6	52.5	36.8	15.0	13.4	29.2	2.1	56.7	46.0	76.3	29.5	65.0	51.8	37.3	39.8	50.3	2.8
	SYNTHIA full-class	9.5	16.3	37.3	-	44.0	-	13.0	10.4	21.8	-	26.2	43.0	65.7	-	59.5	-	35.9	35.1	44.2	-
	SYNTHIA category	23.6	16.5	38.5	-	44.4	-	12.4	9.2	24.1	2.3	48.8	42.7	66.7	-	59.8	-	36.1	33.2	47.9	3.7
KT	Urbansyn full-class	13.7	6.7	44.0	11.8	64.3	5.6	13.0	6.8	20.7	-	43.8	33.5	74.4	19.1	65.3	15.7	37.3	18.9	38.5	-
	Urbansyn category	15.0	6.2	44.8	10.9	79.9	12.1	12.6	6.9	23.6	2.8	49.6	28.4	73.4	17.2	80.5	28.6	33.8	20.0	41.4	2.9
	Synscapes full-class	14.8	5.0	44.8	6.5	17.8	0.5	13.9	5.8	13.6	-	43.1	24.0	75.0	13.0	17.8	1.1	36.6	16.2	28.4	-
	Synscapes category	13.4	4.1	42.6	5.9	45.5	0.6	12.6	5.3	16.3	2.6	39.9	18.9	73.9	12.3	46.0	1.7	35.1	15.8	30.5	2.1
	SYNTHIA full-class	3.0	2.1	32.3	-	32.8	-	2.5	2.9	12.6	-	9.0	12.8	65.2	-	35.7	-	12.0	12.0	24.5	-
	SYNTHIA category	4.9	3.8	35.7	-	36.5	-	2.9	4.5	14.7	2.1	14.3	13.0	70.5	-	39.1	-	13.6	14.2	27.5	3.0

Table 8: Comparison between full-class and category level training. This table shows the performance under full class and category settings on three synthetic datasets: Urbansyn, Synscapes and SYNTHIA. Each dataset is divided into training and validation sets. ‘Src’, ‘CS’ and ‘KT’ evaluation refers to models assessed on their respective source validation sets, Cityscapes and KITTI360, respectively. Notably, the category-level training consistently demonstrates improvements over the full-class counterparts, as highlighted in the Imp. (Improvement) columns. This underscores the effectiveness of our proposed category-based method for generating pseudo-labels.

Our experiments were performed on three synthetic datasets and two real domain datasets to assess the impact of class grouping on instance segmentation accuracy and domain adaptation. For each source domain dataset among UrbanSyn, Synscapes, and SYNTHIA, we split it into a training set and a validation set, with the validation set containing 500 images and the training set comprising the remaining images. Cityscapes validation set contains 500 images, while the KITTI360 validation set comprises 12,276 images.

The results are presented in Table 8. The category training setting consistently outperforms the full-class setting across all evaluation configurations—on the source domain themselves, Cityscapes, and KITTI360. In the source domain evaluation, the category model achieved significant improvements; for example, the UrbanSyn category model improved mAP by 6.3 and mAP50 by 5.9 over the full-class model, while the SYNTHIA category model achieved boosts of 5.9 in mAP and 8.9 in mAP50, respectively. These improvements highlight the effectiveness of the category training approach. In the evaluations on Cityscapes, although the improvements are smaller, the category model still enhances generalization capabilities, with mAP increases of up to 2.9 for UrbanSyn. Similarly, on KITTI360, the category

model consistently outperforms the full-class model, achieving mAP50 gains of up to 3.0. These results suggest that the category training strategy not only improves performance in the source domain but also contributes to better domain adaptation.

The significant performance gains validate our hypothesis that grouping semantically similar classes and training specialized models can enhance instance segmentation accuracy. These findings indicate that semantic class grouping is a viable strategy for improving UDA instance segmentation.

5. Conclusion and Future Work

In this paper, we present a framework named UDA4Inst aiming to provide a strong baseline of synth-to-real UDA for instance segmentation. We incorporate effective UDA methods into the vanilla Mask2Former training protocol: Semantic Category Training and Bidirectional Mixing Training. We show that UDA4Inst achieves significant improvements in instance segmentation compared to the source-only Mask2Former in a comprehensive evaluation of synth-to-real domain settings: from UrbanSyn/Synscapes/SYNTHIA to Cityscapes and KITTI360. Our proposed UDA4Inst model yields state-of-the-art results on SYNTHIA → Cityscapes. This is the first work to provide competitive average precision (AP) results with Synscapes and the recently published synthetic dataset UrbanSyn. For future work, we aim to integrate vision-language foundation models (VFM) into UDA for instance segmentation. VFM models have shown impressive generalization and reasoning capabilities across domains on semantic segmentation, which could be applied to instance segmentation. Preliminary experiments with VFM showed potential that has yet to be explored. Nevertheless, we expect this work to serve as a reference framework for future research in UDA for instance segmentation.

6. Acknowledgements

Antonio M. López acknowledges the financial support to his general research activities given by ICREA under the ICREA Academia Program. Yachan Guo acknowledges the financial support to her PhD from the China Scholarship Council (CSC), grant number 202208310071. All authors acknowledge the support of the Generalitat de Catalunya CERCA Program and its ACCIO agency to CVC’s general activities.

References

- [1] K. Huang, K. Lertniphonphan, F. Chen, J. Li, Z. Wang, Multi-object tracking by self-supervised learning appearance model, in: CVPR Workshops, 2023.
- [2] L. Porzi, M. Hofinger, I. Ruiz, J. Serrat, S. R. Bulo, P. Kortschieder, Learning multi-object tracking and segmentation from automatic annotations, in: CVPR, 2020.
- [3] N. Benbarka, Instance segmentation and 3d multi-object tracking for autonomous driving, Ph.D. thesis, Universität Tübingen (2023).
- [4] J. Chen, M. Sun, T. Bao, R. Zhao, L. Wu, Z. He, 3d model-based zero-shot pose estimation pipeline, arXiv preprint arXiv:2305.17934 (2023).
- [5] L. Aing, W.-N. Lie, G.-S. Lin, Faster and finer pose estimation for multiple instance objects in a single rgb image, Image and Vision Computing 130 (2023) 104618.
- [6] N. Wang, C. Shi, R. Guo, H. Lu, Z. Zheng, X. Chen, Insmos: Instance-aware moving object segmentation in lidar data, arXiv preprint arXiv:2303.03909 (2023).
- [7] P. Li, S. Ding, X. Chen, N. Hanselmann, M. Cordts, J. Gall, Powerbev: A powerful yet lightweight framework for instance prediction in bird's-eye view, in: E. Elkind (Ed.), IJCAI, 2023, pp. 1080–1088.
- [8] M. Cordts, M. Omran, S. Ramos, T. Rehfeld, M. Enzweiler, R. Benenson, U. Franke, S. Roth, B. Schiele, The cityscapes dataset for semantic urban scene understanding, in: CVPR, 2016.
- [9] K.-K. Tseng, J. Lin, C.-M. Chen, M. M. Hassan, A fast instance segmentation with one-stage multi-task deep neural network for autonomous driving, Computers & Electrical Engineering 93 (2021) 107194.
- [10] K. Wong, S. Wang, M. Ren, M. Liang, R. Urtasun, Identifying unknown instances for autonomous driving, in: CoRL, PMLR, 2020.
- [11] S. I. Nikolenko, Synthetic data for deep learning, Vol. 174, Springer, 2021.

- [12] A. Dosovitskiy, G. Ros, F. Codevilla, A. Lopez, V. Koltun, Carla: An open urban driving simulator, in: CoRL, PMLR, 2017.
- [13] C. M. de Melo, A. Torralba, L. Guibas, J. DiCarlo, R. Chellappa, J. Hodges, Next-generation deep learning based on simulators and synthetic data, Trends in cognitive sciences (2022).
- [14] M. Long, Y. Cao, J. Wang, M. Jordan, Learning transferable features with deep adaptation networks, in: ICML, PMLR, 2015.
- [15] Y. Ganin, E. Ustinova, H. Ajakan, P. Germain, H. Larochelle, F. Laviolette, M. March, V. Lempitsky, Domain-adversarial training of neural networks, Journal of machine learning research 17 (59) (2016) 1–35.
- [16] M. Long, Z. Cao, J. Wang, M. I. Jordan, Conditional adversarial domain adaptation, NeurIPS 31 (2018).
- [17] Y. Pan, T. Yao, Y. Li, Y. Wang, C.-W. Ngo, T. Mei, Transferrable prototypical networks for unsupervised domain adaptation, in: CVPR, 2019.
- [18] Z. Lu, Y. Yang, X. Zhu, C. Liu, Y.-Z. Song, T. Xiang, Stochastic classifiers for unsupervised domain adaptation, in: CVPR, 2020.
- [19] Y. Shan, W. F. Lu, C. M. Chew, Pixel and feature level based domain adaptation for object detection in autonomous driving, Neurocomputing 367 (2019) 31–38.
- [20] N. Garnett, R. Uziel, N. Efrat, D. Levi, Synthetic-to-real domain adaptation for lane detection, in: ACCV, 2020.
- [21] J. L. Gómez, G. Villalonga, A. M. López, Co-training for deep object detection: Comparing single-modal and multi-modal approaches, Sensors 21 (9) (2021) 3185.
- [22] P. Oza, V. A. Sindagi, V. V. Sharmini, V. M. Patel, Unsupervised domain adaptation of object detectors: A survey, IEEE TPAMI (2023).
- [23] F. Yu, D. Wang, Y. Chen, N. Karianakis, T. Shen, P. Yu, D. Lymberopoulos, S. Lu, W. Shi, X. Chen, Sc-uda: Style and content gaps aware unsupervised domain adaptation for object detection, in: WACV, 2022.

- [24] G. Mattolin, L. Zanella, E. Ricci, Y. Wang, Confmix: Unsupervised domain adaptation for object detection via confidence-based mixing, in: WACV, 2023.
- [25] M. Biasetton, U. Michieli, G. Agresti, P. Zanuttigh, Unsupervised domain adaptation for semantic segmentation of urban scenes, in: CVPR Workshops, 2019.
- [26] L. Hoyer, D. Dai, L. Van Gool, Daformer: Improving network architectures and training strategies for domain-adaptive semantic segmentation, in: CVPR, 2022.
- [27] L. Hoyer, D. Dai, L. Van Gool, Hrda: Context-aware high-resolution domain-adaptive semantic segmentation, in: ECCV, 2022.
- [28] J. Huang, D. Guan, A. Xiao, S. Lu, L. Shao, Category contrast for unsupervised domain adaptation in visual tasks, in: CVPR, 2022.
- [29] J. L. Gómez, G. Villalonga, A. M. López, Co-training for unsupervised domain adaptation of semantic segmentation models, Sensors 23 (2) (2023) 621.
- [30] J. He, X. Jia, S. Chen, J. Liu, Multi-source domain adaptation with collaborative learning for semantic segmentation, in: CVPR, 2021.
- [31] Z. Liu, Y. Lin, Y. Cao, H. Hu, Y. Wei, Z. Zhang, S. Lin, B. Guo, Swin transformer: Hierarchical vision transformer using shifted windows, in: ICCV, 2021.
- [32] H. Zhang, Y. Tian, K. Wang, H. He, F.-Y. Wang, Synthetic-to-real domain adaptation for object instance segmentation, in: International Joint Conference on Neural Networks (IJCNN), IEEE, 2019.
- [33] J. Huang, D. Guan, A. Xiao, S. Lu, Cross-view regularization for domain adaptive panoptic segmentation, in: CVPR, 2021.
- [34] S. Saha, L. Hoyer, A. Obukhov, D. Dai, L. Van Gool, Edaps: Enhanced domain-adaptive panoptic segmentation, in: Proceedings of the IEEE/CVF International Conference on Computer Vision (ICCV), 2023, pp. 19234–19245.

- [35] B. Cheng, I. Misra, A. G. Schwing, A. Kirillov, R. Girdhar, Masked-attention mask transformer for universal image segmentation, in: CVPR, 2022.
- [36] G. Ros, L. Sellart, J. Materzynska, D. Vazquez, A. M. Lopez, The synthia dataset: A large collection of synthetic images for semantic segmentation of urban scenes, in: CVPR, 2016.
- [37] J. L. Gómez, M. Silva, A. Seoane, A. Borrás, M. Noriega, G. Ros, J. A. Iglesias-Guitian, A. M. López, All for one, and one for all: Urbansyn dataset, the third musketeer of synthetic driving scenes, arXiv preprint arXiv:2312.12176 (2023).
- [38] M. Wrenninge, J. Unger, Synscapes: A photorealistic synthetic dataset for street scene parsing, arXiv preprint arXiv:1810.08705 (2018).
- [39] Y. Liao, J. Xie, A. Geiger, Kitti-360: A novel dataset and benchmarks for urban scene understanding in 2d and 3d, IEEE Transactions on Pattern Analysis and Machine Intelligence 45 (3) (2022) 3292–3310.
- [40] K. He, G. Gkioxari, P. Dollár, R. Girshick, Mask r-cnn, in: ICCV, 2017.
- [41] D. Bolya, C. Zhou, F. Xiao, Y. J. Lee, Yolact: Real-time instance segmentation, in: ICCV, 2019.
- [42] A. Vaswani, N. Shazeer, N. Parmar, J. Uszkoreit, L. Jones, A. N. Gomez, Ł. Kaiser, I. Polosukhin, Attention is all you need, NeurIPS 30 (2017).
- [43] A. Dosovitskiy, L. Beyer, A. Kolesnikov, D. Weissenborn, X. Zhai, T. Unterthiner, M. Dehghani, M. Minderer, G. Heigold, S. Gelly, et al., An image is worth 16x16 words: Transformers for image recognition at scale, arXiv preprint arXiv:2010.11929 (2020).
- [44] H. Zhao, J. Jia, V. Koltun, Exploring self-attention for image recognition, in: CVPR, 2020.
- [45] P. Ramachandran, N. Parmar, A. Vaswani, I. Bello, A. Levskaya, J. Shlens, Stand-alone self-attention in vision models, NeurIPS 32 (2019).
- [46] B. Cheng, A. Schwing, A. Kirillov, Per-pixel classification is not all you need for semantic segmentation, NeurIPS 34 (2021).

- [47] F. Li, H. Zhang, H. Xu, S. Liu, L. Zhang, L. M. Ni, H.-Y. Shum, Mask dino: Towards a unified transformer-based framework for object detection and segmentation, in: CVPR, 2023.
- [48] J. Jain, J. Li, M. T. Chiu, A. Hassani, N. Orlov, H. Shi, Oneformer: One transformer to rule universal image segmentation, in: CVPR, 2023.
- [49] A. Rozantsev, M. Salzmann, P. Fua, Beyond sharing weights for deep domain adaptation, IEEE TPAMI 41 (4) (2018) 801–814.
- [50] B. Sun, J. Feng, K. Saenko, Return of frustratingly easy domain adaptation, in: AAAI, 2016.
- [51] X. Liu, Y. Han, S. Bai, Y. Ge, T. Wang, X. Han, S. Li, J. You, J. Lu, Importance-aware semantic segmentation in self-driving with discrete wasserstein training, in: AAAI, 2020.
- [52] J. Hoffman, D. Wang, F. Yu, T. Darrell, Fcns in the wild: Pixel-level adversarial and constraint-based adaptation, arXiv preprint arXiv:1612.02649 (2016).
- [53] J. Hoffman, E. Tzeng, T. Park, J.-Y. Zhu, P. Isola, K. Saenko, A. Efros, T. Darrell, Cycada: Cycle-consistent adversarial domain adaptation, in: ICML, Pmlr, 2018.
- [54] Y.-H. Tsai, W.-C. Hung, S. Schulter, K. Sohn, M.-H. Yang, M. Chandraker, Learning to adapt structured output space for semantic segmentation, in: CVPR, 2018.
- [55] K. Saito, K. Watanabe, Y. Ushiku, T. Harada, Maximum classifier discrepancy for unsupervised domain adaptation, in: CVPR, 2018.
- [56] R. Gong, W. Li, Y. Chen, L. V. Gool, Dlow: Domain flow for adaptation and generalization, in: CVPR, 2019.
- [57] T.-H. Vu, H. Jain, M. Bucher, M. Cord, P. Pérez, Advent: Adversarial entropy minimization for domain adaptation in semantic segmentation, in: CVPR, 2019.
- [58] L. Hoyer, D. Dai, H. Wang, L. Van Gool, Mic: Masked image consistency for context-enhanced domain adaptation, in: CVPR, 2023.

- [59] W. Tranheden, V. Olsson, J. Pinto, L. Svensson, Dacs: Domain adaptation via cross-domain mixed sampling, in: WACV, 2021.
- [60] S. Lee, J. Hyun, H. Seong, E. Kim, Unsupervised domain adaptation for semantic segmentation by content transfer, in: Proceedings of the AAAI conference on Artificial Intelligence, Vol. 35, 2021, pp. 8306–8315.
- [61] L. Gao, J. Zhang, L. Zhang, D. Tao, Dsp: Dual soft-paste for unsupervised domain adaptive semantic segmentation, in: ACM Multimedia, 2021.
- [62] X. Huo, L. Xie, W. Zhou, H. Li, Q. Tian, Focus on your target: A dual teacher-student framework for domain-adaptive semantic segmentation, in: Proceedings of the IEEE/CVF International Conference on Computer Vision, 2023, pp. 19027–19038.
- [63] D. Kim, M. Seo, K. Park, I. Shin, S. Woo, I. S. Kweon, D.-G. Choi, Bidirectional domain mixup for domain adaptive semantic segmentation, in: AAAI, 2023.
- [64] A. Cardace, P. Z. Ramirez, S. Salti, L. Di Stefano, Shallow features guide unsupervised domain adaptation for semantic segmentation at class boundaries, in: Proceedings of the IEEE/CVF Winter Conference on Applications of Computer Vision, 2022, pp. 1160–1170.
- [65] S. Yun, D. Han, S. J. Oh, S. Chun, J. Choe, Y. Yoo, Cutmix: Regularization strategy to train strong classifiers with localizable features, in: ICCV, 2019.
- [66] T.-Y. Lin, M. Maire, S. Belongie, J. Hays, P. Perona, D. Ramanan, P. Dollár, C. L. Zitnick, Microsoft coco: Common objects in context, in: ECCV, Springer, 2014.
- [67] I. Loshchilov, F. Hutter, Decoupled weight decay regularization, arXiv preprint arXiv:1711.05101 (2017).

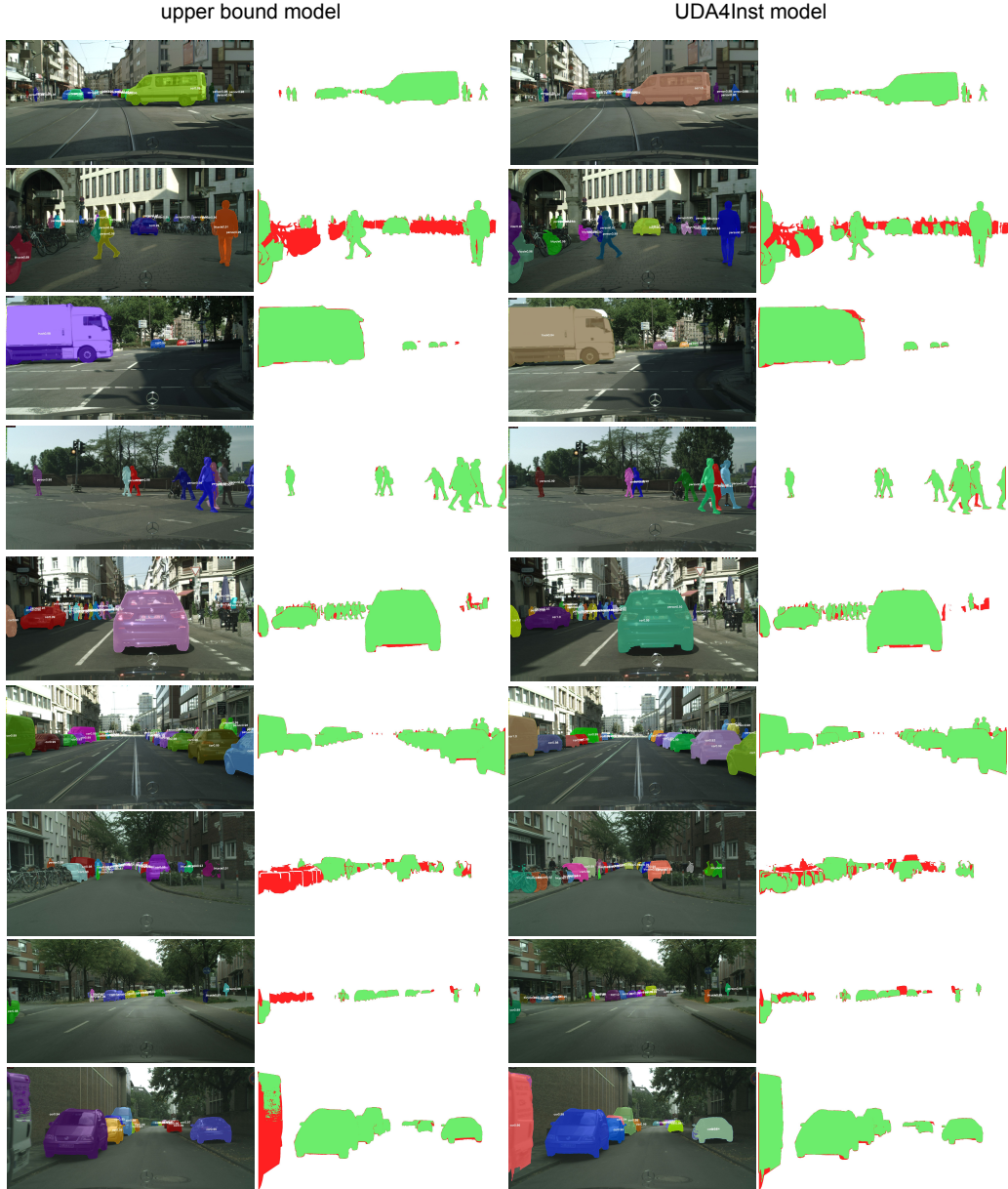


Figure 8: Qualitative comparison of instance segmentation for the upperbound model and UDA4Inst for UrbanSyn → Cityscapes. We show the instance segmentation predictions on images and error maps of semantic results. **Green** indicates correct predictions, while **red** highlights errors compared to the ground truth.